ORIGINAL PAPER

CrossMark

A hybrid drought index combining meteorological, hydrological, and agricultural information based on the entropy weight theory

Jiwei Zhu[1] · Linan Zhou[1] · Shengzhi Huang[1]

Abstract

Drought assessment would be insufficient and unreliable when using the existing indicators based on a single variable (e.g., precipitation) or a combination of two variables (e.g., precipitation and runoff). Therefore, the entropy theory was utilized to develop a hybrid drought index (HDI) that combines meteorological, hydrological, and agricultural information based on precipitation, runoff, and soil moisture data, respectively, and it was applied to characterize the drought condition in Northwest China. Furthermore, the linkages between the atmospheric circulation anomaly/sunspot activities and the HDI series in Northwest China were explored through cross wavelet analysis. The results indicated that (1) HDI has a good performance to capture drought in Northwest China due to its consideration of multiple variables; (2) the annual HDI series in Northwest China was dominated by an insignificantly upward trend, except for Xinjiang, and this trend will be the opposite in the near future; and (3) generally, all of the sunspot activities, El Niño-Southern Oscillation (ENSO) events, AMO (Atlantic Multidecadal Oscillation), and PDO (Pacific Decadal Oscillation) had strong associations with the HDI series in Northwest China, in which sunspot activities had the strongest effects on drought conditions, whereas the AMO had the relatively lowest impacts. This study sheds new light on developing the hybrid drought index, and the findings are valuable for local drought mitigation.

Keywords Hybrid drought index · Entropy weight method · Variable fuzzy set theory · Northwest China

Introduction

Drought is one of the most important natural hazards in the world, and it has a high frequency and wide scope, which has far-reaching impacts on regional economic and ecological environments (Begueria et al. 2010; Vicente-Serrano et al. 2010). The IPCC report (2014) noted out that global climate change resulted in the increase of surface evaporation, latent heat, frequency of drought events, and intensified drought trends (Griggs and Noguer 2002). According to statistics, annual global economic losses caused by drought are approximately US$6–8 billion (Keyantash and Dracup 2002; Wilhite 2000). Even worse, serious drought disasters directly threaten the social stability of a country. The characteristics and causes of drought are critically important to the early warning and risk analysis of drought disaster (Kogan 2000; Hayes et al. 2004).

Drought indices are important tools for analyzing and evaluating drought, when combined with parameters such as moisture deficit ullage. They can determine the drought intensity, the cycle, and the range of time and space (Wilhite 2000). Over the past several decades, a number of different drought indices have been established to assess meteorological drought, agriculture drought, hydrologic drought, and socioeconomic drought (American Meteorological Society 1997; Mishra and Singh 2010). They primarily include the standardized precipitation index (SPI; McKee et al. 1993), Palmer drought severity index (PDSI; Palmer 1965), and crop moisture index (CMI; Palmer 1968). Among these drought indicators, SPI (McKee et al. 1993) is the most commonly used meteorological drought assessment index (Shukla et al. 2011). SPI adopts a gamma distribution to describe the precipitation change rule. It is then transformed into a normal distribution using an equal-probability transformation (McKee et al. 1993; Edwards and McKee 1997; Mishra et al. 2009). SPI is adaptable for analyzing drought at variable timescales with only precipitation data. Although it is simple to characterize drought, SPI tends to lose the connection with ground conditions. Additionally, SPI fails to identify regions with a greater

✉ Shengzhi Huang
huangshengzhi7788@126.com

1 State Key Laboratory of Eco-hydraulics in Northwest Arid Region of China, Xi'an University of Technology, Xi'an 710048, China

tendency to droughts (Zargar et al. 2011). PDSI (Palmer 1965) is another widely recognized drought index (Guttman 1999; Kim et al. 2003) that considers not only precipitation but also evapotranspiration and soil moisture. It is more comprehensive than precipitation and can reflect long-term drought. However, it also has several drawbacks. It regard all precipitation as rainwater. Therefore, it will lead to a loose drought assessment of winter and high altitudes (Mishra and Cherkauer 2010; Mishra and Singh 2010). In addition, there are some assumptions that do not conform to the water balance theory (such as evaporation hypothesis), and its sensitivity to alternate drought is low (Liu et al. 2004; Ma et al. 2015).

In general, most existing available indices are used to evaluate a specific type of drought, such as meteorological drought (rainfall), agriculture drought (soil moisture), and hydrologic drought (runoff) (Heim 2002), leading to an out-sync of the drought onset and termination. A meteorological drought assessed by the shortage in rainfall may develop and end early, whereas the onset and termination of the corresponding hydrologic drought assessed by the deficit in runoff are relatively lagging (Pandey and Ramasastri 2001). This might not be adequate to obtain a comprehensive idea of drought (AghaKouchak 2015). Some scholars developed several comprehensive drought indicators that consider multiple variables by using a parameter method. For example, they derived the bivariate drought indices to quantify drought by using copulas. Kao and Govindaraju (2010) constructed a Joint Drought Index (JDI) that considers both precipitation and streamflow by using a copula. This method provides a new idea of drought assessment that integrates different drought types.

However, this method is not suitable for higher dimensional cases (i.e., more than three variables) due to the lack of flexibility in the structure model (Rajsekhar et al. 2015). Additionally, the application of copulas has a limitation in that the data employed should satisfy an assumption. That is, the data should follow a specific probability density function (PDF) (Huang et al. 2014). This assumption, however, is extremely difficult to meet in reality, which results in a large deviation for the low or high quantiles (Sharma 2000).

To overcome these limitations, this paper introduces the entropy weight method to establish a hybrid drought index that combines meteorological, hydrological, and agricultural information. This method can aggregate the various drought types into a single index. Compared with the variance, entropy can better reflect the input data due to its probability distribution (Ebrahimi et al. 1999). It has been proven that entropy is a better comprehensive evaluation method in evaluating the weight of index objectively (Dionisio et al. 2007; Rajsekhar et al. 2015), which is the major motivation of this study.

Northwest China (this paper refers to five provinces: Shaanxi Province, Qinghai Province, Gansu Province, Xinjiang Province, and Ningxia Province) is located in the middle latitude of the Northern Hemisphere. This region lies inland, far from the ocean, and it is mainly affected by the westerly, Asian monsoon as well as the plateau monsoon. Hence, very little water vapor from over the ocean can reach the area (Li et al. 2011; Dai et al. 2010; Chen et al. 1998). It is one of the driest areas of the same latitude (Gao et al. 2012). The vast majority of the area is in arid and semi-arid climates, with a low average precipitation and high volatility. From the middle of the seventeenth century to the beginning of twentieth century, there have been three drought-prone time zones in China, of which the Northwest is the most serious (Wan et al. 2013). The northwest region is the most prone to drought in China, and the annual losses caused by drought accounted for 4 to 6% of the GDP (Zhang et al. 2015). Some scholars have studied the evolution of drought in the northwest region of China (Huang et al. 2015a, b, c; Wan et al. 2014). However, most of them chose the specific single indices mentioned previously, which were not reliable to characterize the northwest drought with complicated factors. Therefore, it is of great significance to adopt hybrid indicators for the scientific and reliable assessment of drought in Northwest China.

The primary objectives of this study are (1) to establish a new hybrid drought index that integrates hydrological, meteorological, and agricultural information; (2) to fully characterize the drought evolution characteristics including its trend, cycle, and persistence in Northwest China; and (3) to identify the driving factors of drought evolution in Northwest China from the perspective of climate change.

Study area and data

Study area

Northwest China is located in the north and northeast of the Qinghai-Tibet Plateau and lies inland, which is far from the sea. The water supply mainly depends on precipitation from the atmosphere (Yang et al. 2012). This region is surrounded by mountains with a gradually decreasing terrain from west to east. The climate is temperate monsoon climate and temperate continental climate. The mean annual precipitation and air temperature in the area decrease from southeast to northwest (Wei et al. 2014), and their distributions are not uniform. The average precipitation in the mountainous areas varies from 400 to 800 mm, while that in the plain areas is only from 50 to 200 mm (Zhao et al. 2011). To characterize the evolution of drought in the northwest region of China, the region is divided into five regions (Shaanxi, Qinghai, Gansu, Xinjiang, and Ningxia) in accordance with the zoning at the provincial level. The regional location is shown in Fig. 1.

Fig. 1 Location of the Northwest China and its five provinces
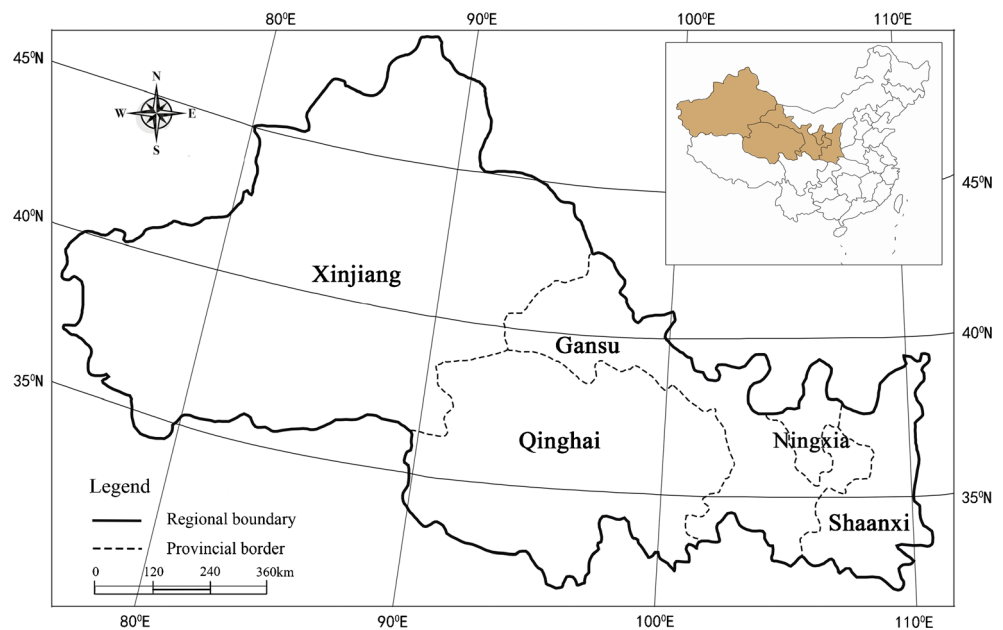
Data

The hydroclimatic variables considered for deriving a comprehensive drought index include the precipitation (P), runoff (R), and soil moisture (SM) for the time period of 1952–2010 on a monthly timescale in Northwest China. The Variable Infiltration Capacity (VIC) (Liang et al. 1994, 1996) model was used to generate the R and SM. The input files required for running the VIC model (e.g., precipitation, wind, speed, and temperature) were acquired from the China Meteorological Administration (CMA) and were interpolated into 0.25°. In the VIC model, total runoff consists of surface runoff and base flow. The soil column is divided into three layers with thicknesses varying from grid cell to grid cell. The VIC model uses the variable infiltration curve to account for the spatial heterogeneity of runoff generation, while vertical movement of moisture through soils follows the 1D Richards equation. Surface runoff from the upper two soil layers is generated when infiltration exceeds the storage capacity of the soil. Base flow is calculated as a function of soil moisture, following the Arno model conceptualization. More details can be found from Liang et al. (1994).

In addition, annual sunspot activity data covering 1952–2010 were obtained from the website http://sidc.oma.be/index.php3). In addition, the Niño 3.4 index data covering 1952–2010 were utilized to examine the correlation between El Niño-Southern Oscillation (ENSO) events and hybrid drought index (HDI) variations. They were acquired from the NOAA Earth System Research Laboratory (http://www.esrl.noaa.gov/psd/data/correlation/nina34.data). The annual Atlantic Multidecadal Oscillation (AMO) series was downloaded from the website http://www.esrl.noaa.gov/psd/gcos_wgsp/Timeseries/AMO/ and annual Pacific Decadal

Oscillation (PDO) data were acquired from the Joint Institute for the Study of the Atmosphere and Ocean (JISAO) (http://jisao.washington.edu/pdo).

Methodologies

Entropy weight method

Entropy was widely used to measure the disorder degree of information in the field of information theory (Lin et al. 2008). The entropy weight is adopted to reflect the difference of the index in different schemes. The higher the entropy weight is, the larger the difference between the index in different scenarios is, and the more useful the information provided for the final decision is. In contrast, the difference of the index in different schemes is less. Entropy reflects the information contained in the objective data. The objectivity reflects how effective the information provided by the index in the evaluation is (Lin et al. 2012). The entropy weight was introduced to provide unbiased relative weights based on the individual variability (Waseem et al. 2015). In an evaluation problem with n evaluating objects and m indicators, the entropy of the ith indicator is expressed as follows:

$$H_i = -k \sum_{j=1}^{n} f_{ij} \ln f_{ij}, i = 1, 2, \ldots, m \qquad (1)$$

where f_{ij} is the frequency of the jth evaluating object in the ith indicator, $f_{ij} = r_{ij} / \sum_{j=1}^{n} r_{ij}$, and $k = 1/\ln n$; if $f_{ij} = 0$, $f_{ij} \ln f_{ij} = 0$. Then, the weight of the entropy of the ith indicator can be expressed as follows:

$$W_i = \frac{1-H_i}{m - \sum\limits_{i=1}^{m} H_i} \tag{2}$$

where $0 \leq W_i \leq 1$ and $\sum_{i=1}^{m} W_i = 1$.

The assessment method for a hybrid drought index based on the variable fuzzy set theory

Assume that an indicator matrix with c grades and m indicators can be expressed as follows:

$$Y = \begin{bmatrix} < a_{12} & [a_{12}, b_{12}] & \cdots & [a_{1(c-1)}, b_{1(c-1)}] & > b_{1(c-1)} \\ > a_{22} & [a_{22}, b_{22}] & \cdots & [a_{2(c-1)}, b_{2(c-1)}] & < b_{2(c-1)} \\ \cdots & \cdots & \cdots & \cdots & \cdots \\ < a_{m2} & [a_{m2}, b_{m2}] & \cdots & [a_{m(c-1)}, b_{m(c-1)}] & < b_{m(c-1)} \end{bmatrix} \tag{3}$$

To conveniently calculate, Eq. (4) was used to transform matrix Y:

$$\begin{cases} y_{i1} = a_{i2} \\ y_{ih} = \dfrac{a_{ih} + b_{ih}}{2}, h = 2, 3, \ldots, (c-1) \\ y_{ic} = b_{i(c-1)} \end{cases} \tag{4}$$

where a_{ih} and b_{ih} are the left and right boundary values of the hth indicator in the ith grade, respectively.

$$Y = \begin{bmatrix} y_{11} & y_{12} & \cdots & y_{1c} \\ y_{21} & y_{22} & \cdots & y_{2c} \\ \cdots & \cdots & \cdots & \cdots \\ y_{m1} & y_{m2} & \cdots & y_{mc} \end{bmatrix} = (y_{ih}) \tag{5}$$

Suppose that x_i of the ith indicator lies in $[y_{ih}, y_{i(h+1)}]$, the relative membership of x_i to the hth grade is calculated as follows:

$$\mu_{ih}(u) = \frac{y_{ih+1}^{-i(h+1)} x_i}{y_{ih+1}^{-i(h+1)} y_{ih}}, h = 1, 2, \ldots, c-1 \tag{6}$$

In addition, the relative membership degree to the rest of grades is zero. Then, the indicator matrix of the relative membership degree can be obtained.

The relative membership degree of evaluating object to h grades is computed as

$$\upsilon_h(u) = \sum_{i=1}^{m} \omega_i * \mu_{ih}(u) \tag{7}$$

where x_i denotes the weight of the ith indicator, and $\sum_{i=1}^{m} \omega_i = 1$. The characteristic value of the evaluating object is calculated as follows:

$$H(u) = \sum_{h=1}^{c} \upsilon_h(u) \times h \tag{8}$$

The Mann-Kendall trend test method

The Mann-Kendall (MK) trend test method is a nonparametric approach and is not affected by the sample value or distribution type (Hamed 2009). Thus, it is recommended by the World Meteorological Organization (Mitchell et al. 1966), and it has been widely used in the trend test of hydrometeorology and other domains (Hamed 2008; Pasquini and Depetris 2011; Kim and Kimball 2012; Huang et al. 2015a, b, c, 2016). Hence, we conducted the Mann-Kendall trend test for the annual HDI series in Northwest China. The detailed procedures for applying the MK can be referred to Hamed (2009). At the α confidence level, if Z is positive, the series has a rising or increasing trend. If not, the series has a declining or decreasing trend. If the absolute value of Z is larger than or equal to 1.64 or 1.96, it means that the time series data meet the confidence level of 90 and 95% in the test trend, respectively.

The rescaled range analysis

The rescaled range (R/S) analysis is a method for processing the time sequence. The basic idea of R/S analysis is to change the timescale of the sample sequence and research its statistical law in different timescales (Oliver and Ballester 1996; Feng et al. 2008).

For a time series of n observations $X = x_1, x_2, \ldots, x_n$, its average series is calculated as follows:

$$y(\tau) = \frac{1}{\tau} \sum_{t=1}^{\tau} x(t) \quad \tau = 1, 2, \ldots \tag{9}$$

where τ denotes the interval and can be any of natural number. Its deviation is calculated as follows:

$$F(t, \tau) = \sum_{t=1}^{\tau} x(t) \quad 1 \leq t \leq \tau. \tag{10}$$

Its range is estimated as follows:

$$R(\tau) = \max_{1 \leq t \leq \tau} F(t, \tau) - \min_{1 \leq t \leq \tau} F(t, \tau) \tag{11}$$

Its standard deviation is calculated as follows:

$$S(\tau) = \left| \frac{1}{\tau} \sum_{t=1}^{\tau} (x(t) - y(\tau))^2 \right|^{1/2} \tag{12}$$

There is a certain linkage between its range and standard deviation:

$$R(\tau)/S(\tau) = (C\tau)^H \tag{13}$$

where C is constant and H denotes the Hurst index.

According to the Hurst exponent of different timescales, the state and law of the time series of the object can be

analyzed. When $H = 0.5$, it means that the time series are independent of each other and are completely random; when $0 < H < 0.5$, it means that the time series has a long-term correlation or persistence but that the future trend of the series will be opposite to the past series. When $H > 0.5$, it indicates that the time series has the characteristics of a long-range correlation and that the process has persistence (Gammel 1998). Therefore, this method can be utilized to analyze the persistence of drought in Northwest China in the near future.

Wavelet analysis

Wavelet analysis is a powerful mathematical tool for non-stationary random signals. It has been widely used to analyze regional climate characteristics and hydrological process due to its properties of local, multi-level, and multi resolutions (Sang and Wang 2008; Xu et al. 2011). The wavelet function $\psi_{a,b}(x)$ can be obtained as follows through the expansion and translation of the mother wavelet $\psi(x)$. The Morlet wavelet was used as the mother wavelet to analyze the hybrid drought index series in this paper, and its expression is as follows:

$$\psi(x) = \frac{1}{\sqrt{2\pi}}\left(1-x^2\right)e^{\frac{-x^2}{2}} \tag{14}$$

where x denotes the hybrid drought index series. The wavelet function is as follows:

$$\psi_{a,b}(x) = \frac{1}{\sqrt{a}}\psi\left(\frac{x-b}{a}\right) \quad a,b \in R, a \neq 0 \tag{15}$$

where a denotes the scale expansion factor and b represents the shift factor. Then, the definition of the continue wavelet transform (CWT) of a signal or function $f(x) \in L^2(R)$ is as follows:

$$W_f(a,b) = \int_R f(x)\psi_{a,b}dx = \frac{1}{\sqrt{a}}\int_R f(x)\psi\left(\frac{x-b}{a}\right)dx \tag{16}$$

where $W_f(a,b)$ is wavelet transform coefficient. Through it, the wavelet transform coefficient map can be obtained. Then, the evolution characteristics of drought conditions in Northwest China can be acquired.

The cross wavelet analysis

The cross wavelet analysis can express the interaction between the vibration components of two time series (Torrence and Compo 1998; Jevrejeva et al. 2003). Based on the wavelet transform of each factor, wavelet coefficients of different factors are multiplying. Then, the cross wavelet spectrum is established. There are two time series X and Y that have wavelet transforms $W_n^X(s)$ and $W_n^Y(s)$, respectively. The cross wavelet transform (XWT) is defined as $W_n^{Y*}(s)$, where $W_n^{XY}(s) = W_n^X(s)W_n^{Y*}(s)$ and is the complex conjugate of $W_n^Y(s)$. The cross wavelet power is further defined as $\left|W_n^{XY}(s)\right|$. The background power spectra of two time series are P_k^X and P_k^Y. The theoretical distribution of the cross wavelet power is given by Torrence and Compo (1998) and is shown as follows:

$$D\left(\frac{W_n^X(s)W_n^{Y*}(s)}{\sigma_X\sigma_Y} < p\right) = \frac{Z_\nu(p)}{\nu}\sqrt{P_k^X P_k^Y} \tag{17}$$

where $Z_\nu(p)$ is the confidence level associated with the probability p for a FDF (filtered density function) defined by the square root of the product of two χ^2 distributions (Grinsted et al. 2004), σ_X and σ_Y are the respective standard deviations (Torrence and Compo 1998). The codes of the cross wavelet transform can be freely downloaded from the following website: http://www.pol.ac.uk/home/research/waveletcoherence/.

Results and discussions

The hybrid drought index

To comprehensively and reliably assess the drought condition, a comprehensive index system of drought assessment was established to evaluate the temporal distribution and change trend of the drought degree that integrated information about the meteorological, hydrological, and agricultural drought. Combined with the actual situation in Northwest China, the precipitation, runoff, and soil moisture anomaly percentage were selected to represent the factors of meteorological, hydrological, and agricultural drought respectively. These three indicators were divided into five grades that ranged from no drought to extreme drought and corresponded to drought levels of 1, 2, 3, 4, and 5, respectively. The detailed drought index system was established and is shown in Table 1, combined with the indicator system referred to Huang et al. (2015a, b, c).

The entropy weights reflect the variations in the degrees of precipitation, runoff, and soil moisture. When the changes in the index series are obvious, their entropies are small and vice versa. The weights in the five provinces of Northwest China were computed based on the entropy weight method and that is presented in Table 2. It can be clearly seen that the monthly runoff anomaly percentage series has the largest weight, whereas the monthly soil moisture anomaly percentage series has the smallest weight in Northwest China. The monthly precipitation anomaly percentage series is lightly less than the runoff. It is concluded that the changes in precipitation and runoff are far more prominent than soil moisture in Northwest China due to the properties of entropy weight.

Table 1   The HDI system of drought assessment in Northwest China

Drought types	Drought indexes	Drought grade				
		ND 1	LD 2	MD 3	SD 4	ED 5
Meteorological drought	APMP (%)	Greater than − 25	(− 25 to − 50)	(−50 to − 70)	(−70 to − 80)	(Less than − 80)
Hydrological drought	APMR (%)	Greater than − 10	(− 10 to − 30)	(−30 to − 50)	(−50 to − 80)	(Less than − 80)
Agricultural drought	APMSM (%)	Greater than − 10	(− 10 to − 30)	(−30 to − 50)	(−50 to − 80)	(Less than − 80)

The APMP, APMR, and APMSM denote anomalous percentage of monthly precipitation, anomalous percentage of monthly runoff, and anomalous percentage of monthly soil moisture, respectively. The ND, LD, MD, SD, and ED denotes no drought, light drought, moderate drought, severe drought, and extreme drought, respectively

Thus, the comprehensive drought indicator primarily contains the information of meteorological and hydrological factors. In general, the changes in runoff and soil moisture in th enorthern area are more obvious than are those in the southern area in Northwest China.

According to the "The assessment method for a hybrid drought index based on the variable fuzzy set theory" and the calculated weights of the meteorological, hydrological, and agricultural factors, the HDI in the five provinces of Northwest China were obtained. To better identify the drought characteristics, the HDI covering 1952–2010 and the linear trend fitting line are plotted and displayed in Fig. 2. It can be easily observed from Fig. 2 that the droughts are relieved in Xinjiang and Qinghai, which is consistent with the finding of Li et al. (2012) and Yang et al. (2013). For the condition in Shaanxi, Gansu, and Ningxia, the observation is the opposite, which implies that the drought conditions have an aggravating trend in the east of Northwest China. This result is similar to that of Cai et al. (2013).

To verify the performance of HDI, historical drought data from the literature and yearbooks were collected and used to compare the drought conditions identified by the developed HDI. From Fig. 2, it can be obviously seen that five provinces in Northwest China suffered from a severe drought disaster in 1957, which is consistent with the record of *China's disaster report: 1949–1995*(Zhang and Fan 1995). Similarly, the *China's disaster report: 1949–1995* indicated that Shaanxi, Gansu, and Ningxia which are located in the east of Northwest China suffered from a severe drought disaster in 1972 that were captured well by HDI (Fig. 2). This demonstrates the value of the HDI and further verifies the reliability of the constructed HDI in charactering drought conditions.

In addition, we calculated the correlation coefficient between HDI and SPI/SRI in Northwest China. The results are shown in Table 3. It can be easily observed from Table 3 that the developed HDI series shows strong correlations with SPI and SRI, which can further prove the reliability of the developed HDI series. Therefore, the developed HDI in this study is a reliable indicator for drought characterization assessment,

and it can be used to examine the drought evolution characteristics in Northwest China.

The temporal trend and persistence of drought

The MK method was used to calculate the temporal trend of drought in Northwest China, and the computed trends of annual HDI are shown in Table 4. All of the MK statistics of drought characteristic values over the years in Northwest China are below the critical value at the 95% significance level. Generally, the annual drought characteristic value is dominated by an insignificant upward trend in Northwest China, which is consistent with Cheng and Wang (2006) and implies that the drought risk of Northwest China is expected to increase to a certain extent. However, the characteristic value over the years in Xinjiang is mainly characterized by an insignificantly decreasing trend, suggesting that the drought risk of Xinjiang has a decreasing tendency to a certain extent.

Through the previous analysis, Northwest China has exhibited a slight drought trend over the last 59 years (1952–2010). Investigating of the persistence of drought in the future is thus important for drought mitigation and early warning in Northwest China. According to "The rescaled range analysis", the R/S analysis was adopted to compute the Hurst indices of the comprehensive drought index series in the five provinces and is displayed in Table 5. Table 5 shows that the Hurst indices of Shaanxi, Qinghai, Gansu, and Ningxia are smaller than 0.5, indicating that the upward

Table 2   The weights of the five provinces in Northwest China based on the entropy theory

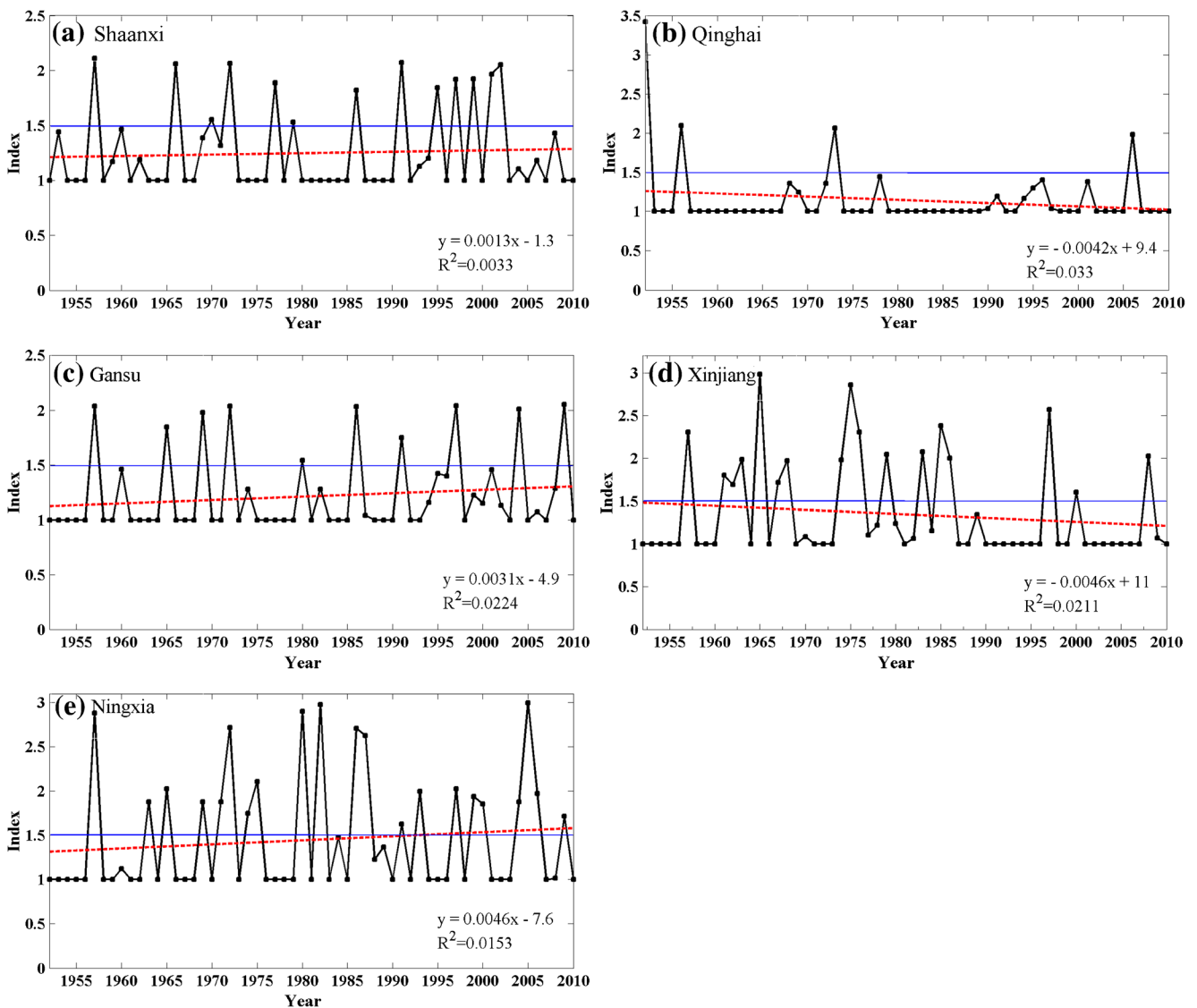| Province	Precipitation	Runoff	Soil moisture
Shaanxi	0.4314	0.5634	0.0052
Qinghai	0.4504	0.5454	0.0042
Gansu	0.4377	0.5586	0.0037
Xinjiang	0.3255	0.6664	0.0081
Ningxia	0.3938	0.5968	0.0095

Fig. 2 The annual HDI curves and its trendlines of in Shaanxi (**a**), Qinghai (**b**), Gansu (**c**), Xinjiang (**d**), and Ningxia (**e**), respectively. The average for previous years is denoted by the black contour (more than is significant, blow is not significant)

trend of HDI will be opposite in the near future, while the Hurst indices value of Xinjiang is equal to 0.5, implying that the change of its HDI series is completely random and has no obvious persistence.

Table 3 The correlation coefficient values between HDI and SPI/SRI in Northwest China

Province	Correlation coefficient with SPI	Correlation coefficient with SRI
Shaanxi	0.6581	0.6910
Qinghai	0.5073	0.5380
Gansu	0.6660	0.6805
Xinjiang	0.6027	0.6570
Ningxia	0.6423	0.6724

The period of dry and wet conditions in Northwest China

To analyze the periodic characteristics of drought in Northwest China, the wavelet transform was adopted to compute the drought period in this study. The wavelet analysis method based on the Morlet wavelet was used and the time–frequency

Table 4 The trends of drought in the five provinces

Province	MK statistics
Shaanxi	0.3989
Qinghai	0.1308
Gansu	1.9226
Xinjiang	− 0.8436
Ningxia	1.1771

Table 5 The persistence of drought in the five provinces

Province	Hurst index
Shaanxi	0.4255
Qinghai	0.4929
Gansu	0.4083
Xinjiang	0.4999
Ningxia	0.4404

distribution of the annual drought characteristic values in Northwest China is illustrated in Fig. 3. This figure reflects the distribution of fluctuating energy in different time and frequency scales. It can be seen that various timescales (cycles) and their intensity (energy size) vary with the scales in a time series (Hu et al. 2010). The red color represents the positive phase, the blue color denotes the negative phase, and the yellow and green colors are between the positive and negative phases. The striking alternation of positive and negative phases represents the alternation of dry and wet conditions. From Fig. 3, it can be obviously seen that a primary period of 32–34 years of

dry and wet conditions occurred in the five provinces. In addition, Xinjiang has a secondary period of approximately 19 years and a third period of approximately 9 years. Ningxia has a secondary period of approximately 19 years and a third period of approximately 5 years. Some scholars deem that some of the large-scale climatic factors have a strong influence on the condition of climate and atmosphere via radiation and magnetic field change (Dou and Yan 2013; Wang et al. 2014; Xu et al. 2015). Thus, the specific linkages between the drought condition in Northwest China and sunspot activities, the Niño3.4 index, and etc. will be investigated in the following section based on the cross wavelet method.

Identification of possible reasons of drought

Sunspot activities, Niño 3.4 index, AMO (Atlantic Multidecadal Oscillation), and PDO (Pacific Decadal Oscillation) are closely associated with the Earth's climate (Van Gee et al. 2002; Glantz et al. 1991; Yu and Zwiers 2007; Knight et al. 2006). Therefore,
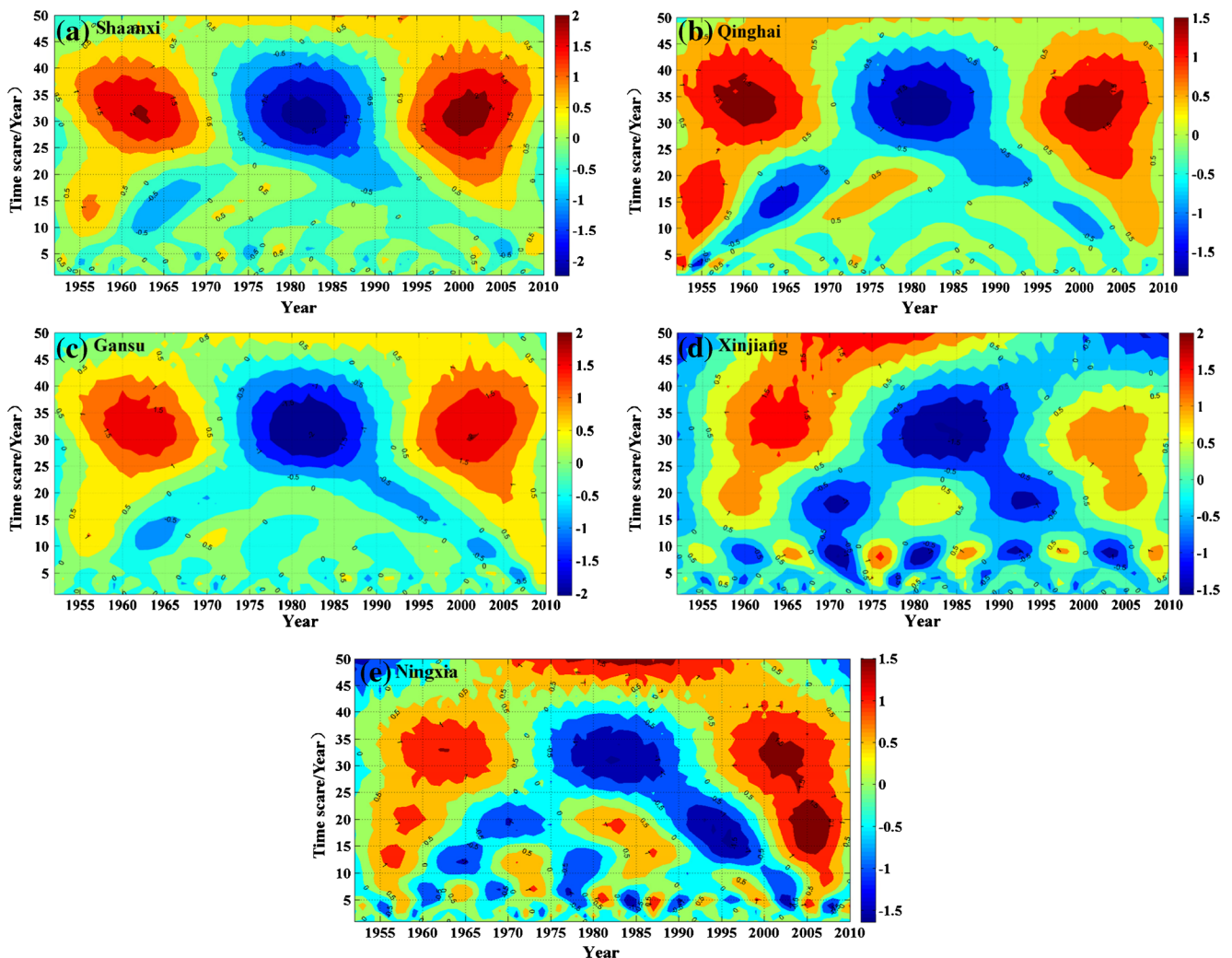

Fig. 3 The time–frequency distribution of the annual HDI in Shaanxi (**a**), Qinghai (**b**), Gansu (**c**), Xinjiang (**d**), and Ningxia (**e**), respectively

the cross wavelet transform with the Morlet wavelet as the mother wavelet was utilized to explore the relationships between the drought variations in Northwest China and the large-scale climatic factors in both the time and frequency domains. Their cross wavelet transforms are shown in Fig. 4. Different colors indicate the relative changes in energy density. The red and blue colors denote the peak and valley values of energy density, respectively. The value within the thick black lines denotes that the correlation is significant at the 95% confidence level.

Sunspot activities have a statistically positive correlation with droughts in Northwest China with a 5- to 11-year signal in 1952–1965 at the 95% confidence level (Fig. 4a). Additionally, sunspot activities have a statistically significant negative correlation with HDI series in this region at the 95% confidence level with a 9- to 14-year signal in 1965–2005, implying that sunspot activities are closely associated with the drought conditions in Northwest China. Similarly, Fig. 4b indicates that the Niño 3.4 has a statistically positive correlation with HDI variations with a 3- to 7-year signal in 1952–1962, a 2- to 4-year signal in 1967–1975, and a 3- to 6-year signal in 1983–1996. These statistically significant positive correlations directly demonstrate that ENSO events play an important role in the causes of drought in Northwest China. In addition, Fig. 4c exhibits that the AMO has a statistically negative correlation with HDI series with a period of 1–2 years in 1952–1960, a period of 2–3 years in 1967–1973, a period of 3–4 years in 1984–1988, and a period of 1–4 years in

1996–2000 at the 95% confidence level, implying that AMO is also closely associated with the drought conditions in Northwest China. Additionally, it can be observed from Fig. 4d that the PDO has a statistically positive correlation with the HDI variations in Northwest China with a 2- to 8-year signal in 1952–1962 and a 2- to 6-year signal in 1983–1998 at the 95% confidence level. Therefore, PDO exerts a strong influence on the drought conditions in Northwest China.

Generally, sunspot activities, ENSO events, AMO, and PDO have strong impacts on triggering drought in Northwest China. Specifically, based on the energy distribution and range from Fig. 4, it can be concluded that the correlation degree of sunspot activities and drought conditions is most obvious, implying that sunspot activities have the strongest effects on drought conditions in Northwest China (Fig. 4a), whereas the effects of ENSO events and PDO are lower than those of sunspot activities (Fig. 4b, c), and those of ENSO are larger than PDO. Relatively, the AMO has the lowest impacts on drought conditions in Northwest China (Fig. 4d).

Conclusions

The onset and termination of droughts are difficult to capture precisely for a traditional drought index based on a single drought variable, because drought indicators are simply defined as periods with a sustained lack of water and can be
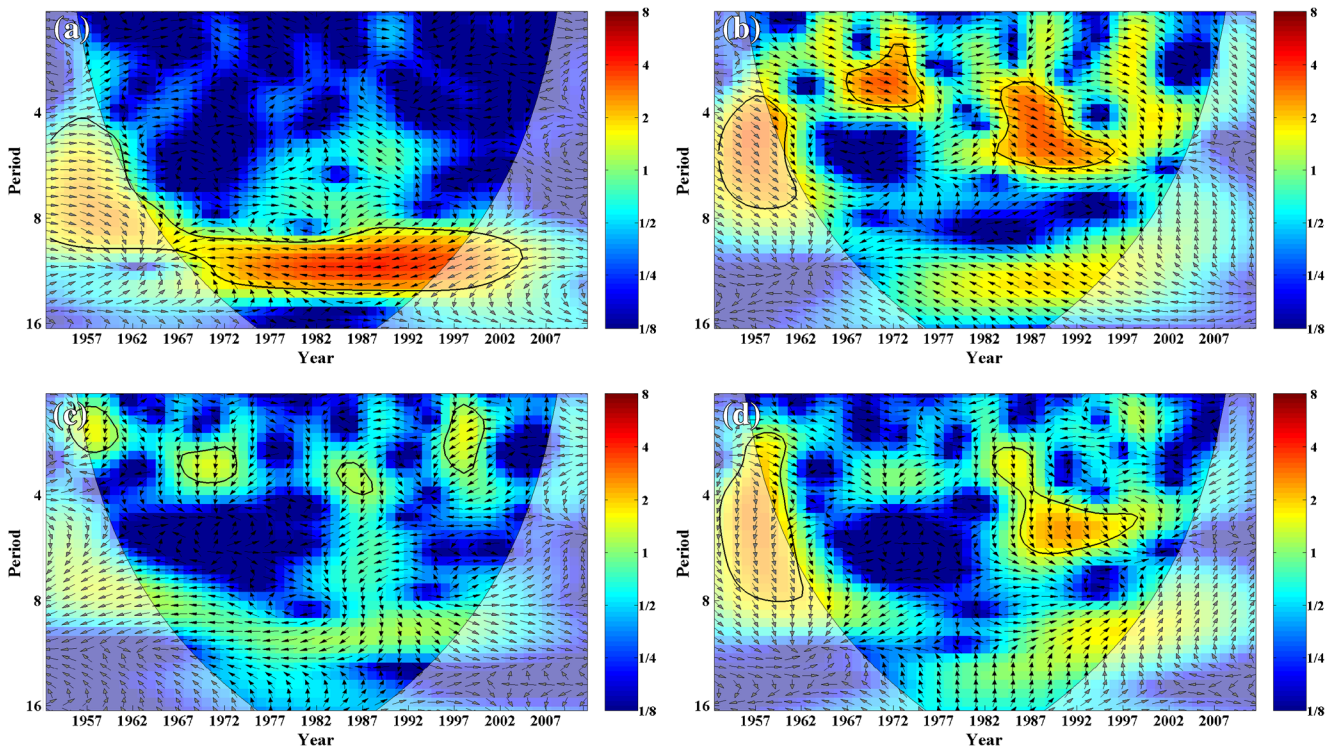

Fig. 4 The cross wavelet transforms between the annual HDI and the sunspot number (**a**), Nino 3.4 index (**b**), AMO (**c**), and PDO (**d**). The thick black contour designates the 5% significance level against red noise, and the arrows denote the relative phase relationship (with in-phase pointing right, anti-phase pointing left)

defined differently (e.g., lack of precipitation, runoff, or soil moisture) (Hao and AghaKouchak 2013). Thus, establishing a reliable multiple drought indicator is important for drought assessment and early warning. In this paper, a hybrid drought index (HDI) was constructed using the variable fuzzy set theory combining meteorological, hydrological, and agricultural drought information, whose weights were objectively determined by using the entropy weight method. The developed HDI was applied to examine the drought evolution characteristics in Northwest China. Further, the temporal trend, persistence, and period of drought were analyzed in this manuscript. Furthermore, the possible causes of the drought evolution in Northwest China were also further explored. The primary conclusions are as follows:

1. Due to its comprehensiveness, HDI is proven to be capable of precisely capturing drought onset by means of comparing to historical drought events that occurred in Northwest China. Therefore, the calculated HDI is a reliable and comprehensive indicator for drought assessment.

    Generally, the annual HDI series in Northwest China is dominated by an insignificantly upward trend except for Xinjiang Province. The result of R/S analysis indicates that the upward trend of HDI will be opposite in the near future, while the drought conditions in Xinjiang are completely random and have no obvious persistence.

2. The annual HDI in Northwest China has a striking periodic variation. A primary period of 32–34 years of drought and wet conditions was observed in the whole region, while Xinjiang has another two periods of approximately 19 and 9 years, and Ningxia also has another two periods of approximately 19 and 5 years.

3. In general, all of the sunspot activities, Niño 3.4 index, AMO, and PDO have strong associations with the HDI series in Northwest China, in which sunspot activities had the strongest effects on drought conditions, while the AMO had the relatively lowest impacts. These factors can be used as input variables for drought prediction due to their correlations with the drought conditions, thus improving the accuracy of drought forecasting.

In general, this study sheds new light on developing a hybrid drought index by means of the entropy weight theory, and the findings are valuable for local drought mitigation. In this paper, Northwest China was selected as a case study, and the developed HDI can also be applied in other regions of the world. There are also some shortcomings of HDI. The most important one is the uncertainty of soil moisture data based on the simulation of the VIC model. Its accuracy is affected by the limited observation stations to a certain extent. We will further improve its accuracy in the future work with more observation stations, thus reducing the uncertainty of the developed HDI series.

References

AghaKouchak A (2015) A multivariate approach for persistence-based drought prediction: application to the 2010–2011 East Africa drought. J Hydrol 526:127–135

American Meteorological Society (1997) Meteorological drought—policy statement. Bull Am Meteorol Soc 78:847–849

Begueria S, Vicente-Serrano SM, Angulo-Martinez M (2010) A multiscalar global drought dataset: the SPEIbase: a new gridded product for the analysis of drought variability and impacts. Bull Am Meteorol Soc 91:1351–1354

Cai XL, Ye DX, Li Q et al (2013) Analysis of temporal-spatial variation characteristics of drought in Shaanxi Province based on compound meteorological drought index (CI). Agric Res Arid Areas 31(5):1–8 (in Chinese)

Chen LX, Zhu WQ, Wang W et al (1998) Studies on climate change in China in recent 45 years. Acta Meteor Sin 1:1–17 (in Chinese)

Cheng GD, Wang GX (2006) Changing trend of drought and drought disaster in northwest China and countermeasures. Earth Sci Front 13(1):3–14 (in Chinese)

Dai Y, Luo Y, Li XP (2010) Review of climate change in the journal Nature 2009. Adv Clim Chang Res 6(2):154–156 (in Chinese)

Dionisio A, Menezes R, Mendes DA (2007) Entropy and uncertainty analysis in financial markets. Appl Phys Finance Anal 4–7 July, Portugal

Dou RY, Yan JP (2013) Relationships between drought and flood disasters in Guanzhong plain and the activities of sunspot. J Arid Land Resour Environ 27(08):76–82 (in Chinese)

Ebrahimi N, Maasoumi E, Soofi ES (1999) Ordering univariate distributions by entropy and variance. J Econ 90(2):317–336

Edwards DC, McKee TB (1997) Characteristics of 20th century drought in the United States at multiple scales. Atmospheric Science Paper No. 634, May 1–30

Feng XL, Feng ZL, Luo LC et al (2008) Fractal analysis of climate change and Hurst index experiment in Tibetan Plateau in future. Arid Land Geogr 31(2):175–181 (in Chinese)

Fifth Assessment Report of the Intergovernmental Panel on Climate Change 2014. Climate change 2014: mitigation of climate change (vol. 3). Cambridge University Press

Gammel BM (1998) Hurst's rescaled range statistical analysis for pseudorandom number generators used in physical simulations. Phys Rev E 58(2):2586–2597

Gao X, Bai HY, Zhang SH et al (2012) Climatic change tendency in Qinling Mountains from 1959 to 2009. Bull Soil Water Conserv 32(1):207–211 (in Chinese)

Glantz MH, Katz RW, Nicholls N (1991) Teleconnections linking world wide climatic anomalies, vol 535. Cambridge University Press, Cambridge

Griggs DJ, Noguer M (2002) Climate change 2001: the scientific basis. Contribution of working group I to the third assessment report of the intergovernmental panel on climate change. Weather 57(8):267–269

Grinsted A, Moore JC, Jevrejeva S (2004) Application of the cross wavelet transform and wavelet coherence to geophysical time series. Nonlinear Process Geophys 11(5/6):561–566

Guttman NB (1999) Accepting the standardized precipitation index: a calculation algorithm. J Am Water Resour Assoc 35(2):311–322

Hamed KH (2008) Trend detection in hydrologic data: the Mann–Kendall trend test under the scaling hypothesis. J Hydrol 349(3):350–363

Hamed KH (2009) Exact distribution of the Mann–Kendall trend test statistic for persistent data. J Hydrol 365(1):86–94

Hao Z, AghaKouchak A (2013) Multivariate standardized drought index: a parametric multi-index model. Adv Water Resour 57:12–18

Hayes MJ, Wilhelmi OV, Knutson CL (2004) Reducing drought risk: bridging theory and practice. Nat Hazard Rev 5(2):106–113

Heim Jr RR (2002) A review of twentieth-century drought indices used in the United States. Bull Am Meteorol Soc 83(8):1149

Hu NF, Wang AZ, Guan DX, Yuan FH, Jin CJ, Wu JB, Wang JJ (2010) Multiple time scale analysis of precipitation series in Changbai Mountain Region in 1959–2006. Chin J Appl Ecol 21(3):549–556 (in Chinese)

Huang SZ, Chang JX, Huang Q et al (2014) Spatio-temporal changes and frequency analysis of drought in the Wei river basin, China. Water Resour Manag 28(10):3095–3110

Huang SZ, Chang JX, Leng GY et al (2015a) Integrated index for drought assessment based on variable fuzzy set theory: a case study in the Yellow River basin, China. J Hydrol 527:608–618

Huang SZ, Huang Q, Chang JX, Zhu Y, Leng G, Xing L (2015b) Drought structure based on a nonparametric multivariate standardized drought index across the Yellow River basin, China. J Hydrol 530: 127–136

Huang XY, Li YH, Feng JY et al (2015c) Climate characteristics of precipitation and extreme drought events in Northwest China. Acta Ecol Sin 35(5):1359–1370 (in Chinese)

Huang SZ, Huang Q, Leng GY, Liu SY (2016) A nonparametric multivariate standardized drought index for characterizing socioeconomic drought: a case study in the Heihe River basin. J Hydrol 542:875–883

Jevrejeva S, Moore JC, Grinsted A (2003) Influence of the Arctic Oscillation and El Nino Southern Oscillation (ENSO) on ice conditions in the Baltic Sea: the wavelet approach. J Geophys Res: Atmos 108(D21):1–12

Kao SC, Govindaraju RS (2010) A copula-based joint deficit index for droughts. J Hydrol 380(1):121–134

Keyantash J, Dracup JA (2002) The quantification of drought: an evaluation of drought indices. Bull Am Meteorol Soc 83(8):1167–1180

Kim Y, Kimball JS, Zhang K et al (2012) Satellite detection of increasing Northern Hemisphere non-frozen seasons from 1979 to 2008: implications for regional vegetation growth. Remote Sens Environ 121:472–487

Kim TW, Valdés JB, Yoo C (2003) Nonparametric approach for estimating return periods of droughts in arid regions. J Hydrol Eng 8(5): 237–246

Knight JR, Folland CK, Scaife AA (2006) Climate impacts of the Atlantic multidecadal oscillation. Geophys Res Lett 33(17):1–14

Kogan FN (2000) Contribution of remote sensing to drought early warning. Early warning systems for drought preparedness and drought management. pp 75–87

Li SS, Hong S, Liu XJ (2011) World climate change research trends. Adv Clim Chang Res 7(1):73–76 (in Chinese)

Li JF, Zhang Q, Chen XH et al (2012) SPI-based drought variations in Xinjiang, China. J Appl Meteorol Sci 23(3):322–330 (in Chinese)

Liang X, Lettenmaier DP, Wood EF, Burges SJ (1994) A simple hydrologically based model of land surface water and energy fluxes for GSMs. J Geophys Res: Atmos 99(D7):14415–14428

Liang X, Lettenmaier DP, Wood EF (1996) One-dimensional statistical dynamic representation of subgrid spatial variability of precipitation in the two-layer variable infiltration capacity model. J Geophys Res: Atmos 101(D16):21403–21422

Lin JK, Jiang YM, Zheng WH et al (2008) Automatic establishment of the initial black start schemes for power systems. Autom Electr Power Syst 32(2):72–75 (in Chinese)

Lin JK, Li TF, Zhao ZM et al (2012) Assessment on power system black-start schemes based on entropy-weighted fuzzy comprehensive evaluation model. Power Syst Technol 36(2):115–120 (in Chinese)

Liu GS, Guo AH, An SQ (2004) Research progress in Palmer drought severity index and it's application. J Nat Disasters 13(4):21–27 (in Chinese)

Ma M, Ren L, Singh VP, Tu X, Jiang S, Liu Y (2015) Evaluation and application of the SPDI-JDI for droughts in Texas, USA. J Hydrol 521:34–45

McKee TB, Doesken NJ, Kleist J (1993) The relationship of drought frequency and duration to time scales. In Proceedings of the 8th Conference on Applied Climatology. Boston, MA: American Meteorological Society 17(22):179–183

Mishra V, Cherkauer KA (2010) Retrospective droughts in the crop growing season: implications to corn and soybean yield in the Midwestern United States. Agric For Meteorol 150(7):1030–1045

Mishra AK, Singh VP (2010) A review of drought concepts. J Hydrol 391(1):202–216

Mishra AK, Singh VP, Desai VR (2009) Drought characterization: a probabilistic approach. Stoch Env Res Risk A 23(1):41–55

Mitchell JM, Dzerdzeevskii B, Flohn H et al (1966) Climate change. WHO Technical Note 79

Oliver R, Ballester JL (1996) Rescaled range analysis of the asymmetry of solar activity. Sol Phys 169(1):215–224

Palmer WC (1965) Meteorological drought, Rep. 45. U.S. Dept. of Commerce, Washington, D.C, pp 58

Palmer WC (1968) Keeping track of crop moisture conditions, nationwide: the new crop moisture index. Weatherwise 21:156–161. https://doi.org/10.1080/00431672.1968.9932814

Pandey RP, Ramasastri KS (2001) Relationship between the common climatic parameters and average drought frequency. Hydrol Process 15(6):1019–1032

Pasquini AI, Depetris PJ (2011) Southern patagonia's perito moreno glacier, Lake Argentino, and Santa Cruz River hydrological system: an overview. J Hydrol 405(1):48–56

Rajsekhar D, Singh VP, Mishra AK (2015) Multivariate drought index: an information theory based approach for integrated drought assessment. J Hydrol 526:164–182

Sang YF, Wang D (2008) Wavelets selection method in hydrologic series wavelet analysis. Shuili Xuebao 39(3):295–300 (in Chinese)

Sharma A (2000) Seasonal to interannual rainfall probabilistic forecasts for improved water supply management: part 1—a strategy for system predictor identification. J Hydrol 239(1):232–239

Shukla S, Steinemann AC, Lettenmaier DP (2011) Drought monitoring for Washington State: indicators and applications. J Hydrometeorol 12(1):66–83

Torrence C, Compo GP (1998) A practical guide to wavelet analysis. Bull Am Meteorol Soc 79(1):61–78

Van Gee B, Raspopov OM, Renssen H et al (2002) The role of solar forcing upon climate change. Climate Change: Natural forcing factors for climate change timescales 10–1 to 10–5 years18, 100

Vicente-Serrano SM, Beguería S, López-Moreno JI (2010) A multiscalar drought index sensitive to global warming: the standardized precipitation evapotranspiration index. J Clim 23(7):1696–1718

Wan JH, Tan XM, Liu CD (2013) Spatial-temporal pattern of drought hazards in China's Qing dynasty based on Forbidden City archives. Adv Water Sci 24(1):18–23 (in Chinese)

Wan JH, Lyu J, Liu HP et al (2014) Drought-flood variation characteristics and trends in arid Northwestern China during 1470–2008. Adv Water Sci 25(5):625–631 (in Chinese)

Wang YM, Feng Q, Li ZX (2014) Analysis of low cloud amount variations in the Northwest China during 1960–2005. Sci Geogr Sin 34(5):635–640 (in Chinese)

Waseem M, Ajmal M, Kim TW (2015) Development of a new composite drought index for multivariate drought assessment. J Hydrol 527: 30–37

Wei ZF, Ren ZY, Zhang C et al (2014) Changes of vegetation cover and its correlation with precipitation and temperature in Northwest China. Bull Soil Water Conserv 34(03):283–289 (in Chinese)

Wilhite DA (2000) Drought as a natural hazard: concepts and definitions. In: Wilhite DA (ed) Drought: a global assessment, hazards disasters Ser, vol I. Routledge, New York, pp 3–18

Xu J, Chen Y, Lu F, Li W, Zhang L, Hong Y (2011) The nonlinear trend of runoff and its response to climate change in the Aksu River, western China. Int J Climatol 31(5):687–695

Xu XY, Zhu JW, Xie JC et al (2015) Evolution characteristics of drought/flood disasters in Xi'an Region from 1951 to 2012 and their correlation to related multiple events. J Nat Disasters 24(6):64–71 (in Chinese)

Yang Q, Qin ZH, Wang T et al (2012) Characteristics of climate factor change in Yulin Region during 1970–2010. Arid Land Geogr 35(5):695–707 (in Chinese)

Yang D, Wang H, Cheng JQ et al (2013) Climate change in Qinghai and its relationship with ENSO in the recent 50 years. Ecol Environ Sci 22(4):547–553 (in Chinese)

Yu B, Zwiers FW (2007) The impact of combined ENSO and PDO on the PNA climate: a 1,000-year climate modeling study. Clim Dyn 29(7–8):837–851

Zargar A, Sadiq R, Naser B et al (2011) A review of drought indices. Environ Rev 19(NA):333–349

Zhang S, Fan BJ (1995) China disaster report (1949–1995) (in Chinese)

Zhang Q, Yao YB, Li YH et al (2015) Research progress and prospect on the monitoring and early warning and mitigation technology of meteorological drought disaster in northwest China. Adv Earth Science 30(2):196–213 (in Chinese)

Zhao CC, Wang Y, Ding YJ et al (2011) Spatial-temporal variations of temperature and precipitation in northern China in recent 50 years. Plateau Meteorol 30(2):385–390 (in Chinese)